Journal Pre-proofs

Well-defined meso/macroporous materials as a host structure for methane hydrate formation: Organic versus carbon xerogels

C. Cuadrado-Collados, J. Farrando-Pérez, M. Martínez-Escandell, L.A. Ramírez-Montoya, J.A. Menéndez, A. Arenillas, M.A. Montes-Morán, J. Silvestre-Albero

PII: S1385-8947(20)32404-9
DOI: https://doi.org/10.1016/j.cej.2020.126276
Reference: CEJ 126276

To appear in: *Chemical Engineering Journal*

Received Date: 5 June 2020
Revised Date: 10 July 2020
Accepted Date: 11 July 2020

Please cite this article as: C. Cuadrado-Collados, J. Farrando-Pérez, M. Martínez-Escandell, L.A. Ramírez-Montoya, J.A. Menéndez, A. Arenillas, M.A. Montes-Morán, J. Silvestre-Albero, Well-defined meso/macroporous materials as a host structure for methane hydrate formation: Organic versus carbon xerogels, *Chemical Engineering Journal* (2020), doi: https://doi.org/10.1016/j.cej.2020.126276

Well-defined meso/macroporous materials as a host structure for methane hydrate formation: Organic versus carbon xerogels

C. Cuadrado-Collados,[1] J. Farrando-Pérez,[1] M. Martínez-Escandell,[1] L.A. Ramírez-Montoya,[2] J.A. Menéndez,[2] A. Arenillas,[2] M.A. Montes-Morán,[2] J. Silvestre-Albero[1,*]

[1]Laboratorio de Materiales Avanzados (LMA), Departamento de Química Inorgánica-IUMA, Universidad de Alicante, 03690 San Vicente del Raspeig, Spain
[2]Instituto de Ciencia y Tecnología del Carbono, INCAR-CSIC, Francisco Pintado Fe 26, 33011 Oviedo, Spain

ABSTRACT

A series of xerogels with a properly designed porous structure and surface chemistry have been synthesized and evaluated as a host structure to promote the nucleation and growth of methane hydrates. Organic xerogels (OGs) have been synthesized from resorcinol-formaldehyde mixtures using a sol-gel approach and microwave heating. These xerogels are hydrophilic in nature and possess designed meso/macrocavities in the pore size range 5-55 nm. Carbon xerogels (CGs) have been synthesized from their organic counterparts after a carbonization treatment at high temperature. Interestingly, the carbonization process does not alter/modify substantially the porous network of the parent xerogels, while developing new micropores. Under water-supplying conditions, the two types of xerogels exhibit a large improvement in the methane adsorption capacity compared to the pure physisorption process taking place in dry conditions (up to 200% improvement), and associated with a significant hysteresis loop. These excellent values must be associated with the promoting effect of these xerogels in the water-to-hydrate conversion process. The comparison of OGs and CGs as a host structure anticipates that surface chemistry, total pore volume and pore size are critical parameters defining the extent and yield of the methane hydrate formation process.

INTRODUCTION

In the last few years there has been a growing interest in the use of methane hydrates as an alternative storage media for natural gas, the so-called solid natural gas (SNG). Methane hydrates are crystalline structures characterized by a large volumetric storage capacity (up to 180 volume of CH_4 gas/volume of CH_4 hydrate) [1]. These structures are mainly located in sub-oceanic sediments at the water continental margins and at the Arctic permafrost and constitute the largest reserves of natural gas, with roughly twice the carbon contained in all conventional reserves of coal, natural gas and oil combined. In terms of composition, gas hydrates are constituted by water molecules joined together through hydrogen bonding, giving rise to a 3D network with free cavities able to host up to one methane molecule per cavity. Under fully occupation conditions, the theoretical stoichiometry is 1 CH_4 molecule per 5.75 H_2O molecules.

In nature, hydrates exhibit a cubic sI structure and contain two different types of cages: i) six large cages containing twelve pentagonal and two hexagonal faces ($5^{12}6^2$) and ii) two small cages having twelve pentagonal faces (5^{12}), with a unit cell lattice parameter of 1.2 nm [1].

Interestingly, these crystalline structures can be artificially synthesized under high-pressure and low temperature conditions. Compared to liquified natural gas (LNG) and compressed natural gas (CNG), storage of natural gas in the form of gas hydrates (SNG) can be considered as a promising alternative to minimize the traditional drawbacks (economical and safety issues) associated with LNG and CNG technologies [2] . One of the main goals with artificial gas hydrates to be technically viable is to overcome the kinetic limitations traditionally associated with the limited gas-liquid reactive interphase [3]. Among the different alternatives to improve the water-to-hydrate yield, one of the most promising ones has been the incorporation in the synthesis media of porous solids with an extended surface area [4-10]. High-surface area nanoporous materials such as activated carbons, silicas, zeolites and metal-organic frameworks (MOFs) have been evaluated as promising host structures to promote the nucleation and growth of gas hydrates. Under confinement conditions, gas hydrates can be grown under milder conditions than nature, and the most important, with faster kinetics [4]. The promoting effect in the confined nanospace of porous solids has been corroborated by Yu and coworkers using molecular dynamic simulations [11]. Despite these promising results achieved so far, there is an urgent need to identify the real role of the porous structure and surface chemistry in these nucleation processes. Previous studies reported in the literature have anticipated that the particle size and the porous network are critical parameters defining the hydrate yield [12,13]. Furthermore, these studies have shown that the presence of cavities in the mesoporous range gives rise to a larger improvement in the amount stored under water supplying conditions compared to the dry system. On the contrary, the role of the surface chemistry is still unclear.

Taking into account the difficulties to study these two parameters at once due to the different chemical nature of the evaluated porous materials (e.g., carbons, silicas, zeolites and MOFs) and the difficulty to stablish specific correlations among them, the main goal of the present manuscript is to overcome these drawbacks through the comparison of two series of xerogels, organic and carbon xerogels, with a relatively narrow macro or mesoporous structure and well-defined surface chemistry. One of the main advantages of xerogels compared to other nanoporous solids is the possibility to tune their porous structure through the modification of the synthesis conditions. In these materials the inner porous structure can be divided into: i) cavities within the clusters, usually with a diameter below 2 nm (micropores), and ii) cavities between clusters, with a diameter in the macro and/or mesoporous range (up to 2000 nm).

Consequently, macro and/or mesocavities can be easily tuned by controlling the amount and size of the clusters formed during the polycondensation reaction [14-16]. This inherent peculiarity opens the gate towards the design of a perfectly tailored porous structure through the modification of the synthesis parameters, i.e. amount of solvent, solution pH, catalysts used, etc. The preparation of the carbon xerogels from their organic counterparts will be performed under perfectly controlled conditions to preserve the macro or mesoporous network of the original OGs, while developing microporosity and changing the surface chemistry of the materials (from hydrophilic to hydrophobic). These two sets of samples will allow to identify, at once, the effect of the porous network and the role of the surface chemistry in the nucleation process under confined environment.

EXPERIMENTAL SECTION

Synthesis of adsorbents

Organic xerogels (OGs) were synthetized from resorcinol (R) (Indspec, 99.6% purity) /formaldehyde (F) (Merck, 37% aqueous solution, including 0.7% methanol, MeOH) solutions in water following a well-established route assisted by microwave heating [14-16]. The use of microwaves in both the curing and drying steps shortens significantly the time of synthesis. As detailed elsewhere [14,15], four parameters are crucial in determining the macro or mesoporosity of the resulting gels, namely the R/F ratio; the so-called dilution (D), which is the molar ratio between total solvents (i.e., water and MeOH) and reactants; the pH of the solution; and the content of MeOH in the initial solution. NaOH was added to increase the pH of the solutions. Normapur MeOH (>99.9 % purity) from VWR Chemicals was added to attain the desired MeOH content. Three different conditions were used to prepare OGs covering the mesopores range (Table 1). Materials in Table 1 were labeled after their average mesopore size in nm.

Table 1. Synthesis conditions for the organic gels.

Sample	pH	R/F	D	% MeOH
OG-5	6.5	0.5	4.7	20
OG-18	6	0.3	5.3	10
OG-55	5.4	0.3	8.0	10

Last but not least, organic gels (ca. 20 g) were carbonized in a horizontal oven at 1073 K under a N_2 flow of 100 ml/min to obtain their carbon counterparts. The carbonized gel particles (CGs)

were cooled down to room temperature under the same nitrogen flow rate and finally milled and sieved down to 1 mm particle size. From Figure 3, the appearance of the organic gels (OGs) together with its carbonized counterparts (CGs) can be appreciated.

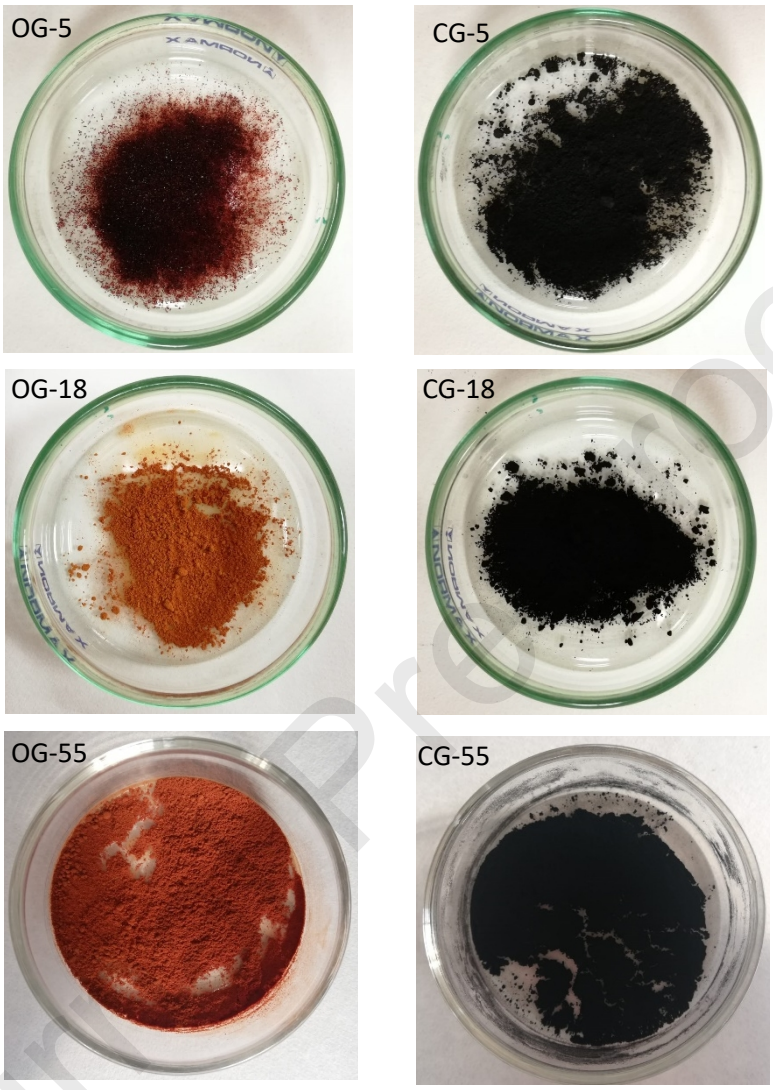

Fig. 3. Images of the physical appearance of the evaluated samples.

Physico-chemical characterization

Textural characteristics of the synthesized xerogels were evaluated by nitrogen adsorption at cryogenic temperatures. N_2 adsorption/desorption isotherms were performed at 77 K using a home-made fully automated manometric equipment designed and developed by the LMA group. Prior to the adsorption measurements, samples (*ca.* 100 mg) were outgassed under ultra-high vacuum at 393 K overnight. Apparent surface area was obtained after application of the BET equation, and total pore volume was deduced from the amount adsorbed at p/p_0= 0.97.

Micropore volume (V_{micro}) was obtained after application of the Dubinin-Radushkevich (DR) equation to the nitrogen adsorption data, and mesopore volume (V_{meso}) was obtained from the difference between V_{total}-V_{micro} [17]. Wider pores were evaluated using mercury porosimetry. These experiments were performed using a Poremaster-60GT equipment from Quantachrome Instruments (amount of samples *ca.* 10 mg).

Water adsorption isotherms were performed at 298K using a home-made manometric equipment designed and constructed by the LMA research group and now commercialized by Quantachrome Instruments as VStar. Before the water adsorption measurements, samples were outgassed under vacuum at 393 K overnight.

Field emission scanning electron microscopy (FESEM) measurements were performed using a Hitachi S3000N microscope. Elemental analysis was performed using a Thermo Finningan Flash 1112 series with a Microelemental Analyser. X-ray diffraction analyses were performed using a Bruker D8-Advanced equipment equipped with a Goebel mirror, a high temperature chamber and an X-ray generator (KRISTALLOFLEX K 760-80F) with a copper anode tube. XRD patterns were acquired between 5 and 80° (2θ) with a step size of 0.05° and a step exposure of 3 s.

High-pressure methane adsorption measurements were performed in a homemade fully automated manometric equipment designed and constructed by the LMA research group and now commercialized as iSorbHP by Quantachrome Instruments. CH_4 adsorption capacity was measured at 295 K and up to 10 MPa for both dry and wet samples. Dry samples were outgassed at 393 K for 12h, while wet samples were frozen at 258 K before the outgassing treatment to avoid water losses. In the specific case of the methane hydrates, samples were pre-adsorbed with distilled water by adding droplets up to the total pore volume provided by the nitrogen isotherms (V_T), i.e. samples were saturated with ultrapure water. To minimize kinetic restrictions, high-pressure methane isotherms were performed under strict equilibrium conditions, a complete isotherm lasting *ca.* 2-3 weeks.

RESULTS AND DISCUSSION

Physico-chemical characterization of the synthesized samples

One of the critical aspects in this study is the evaluation of the porous structure of the synthesized organic xerogels, and to identify how this porous network is altered/modified after a carbonization treatment at high temperature. To this end, the three organic xerogels (OGs) and their carbonized counterparts (CGs) have been evaluated using N_2 sorption at cryogenic temperatures (Figure 4a and 4b, respectively).

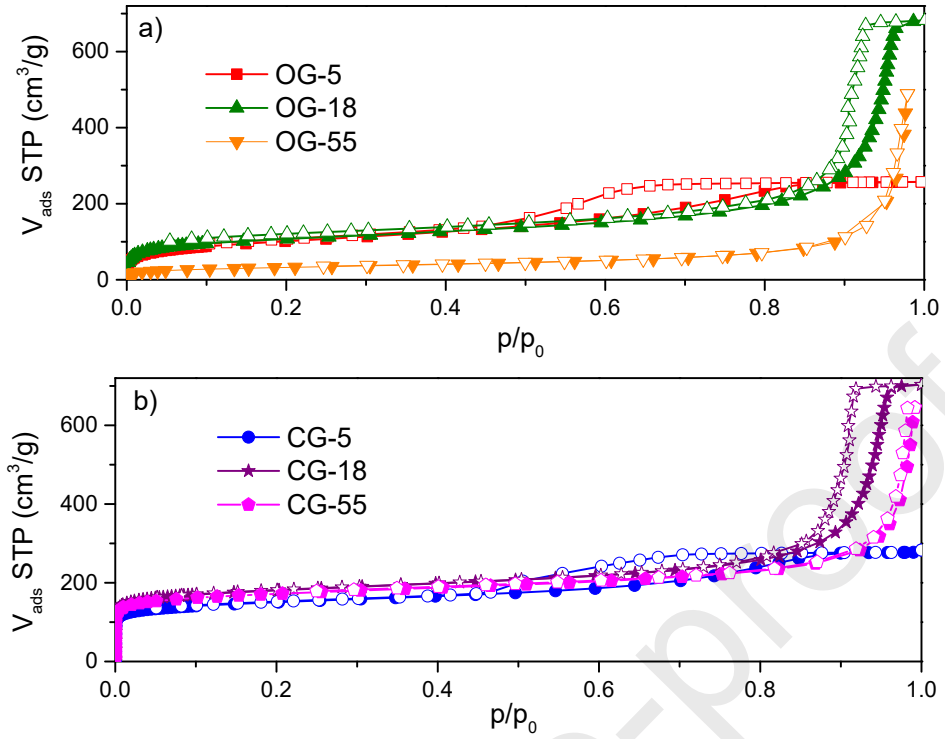

Figure 4. N_2 adsorption (full symbols)/desorption (open symbols) isotherms at 77K for a) organic xerogels and b) carbon xerogels.

As it can be seen, the reported isotherms clearly identify important differences among samples in terms of porous structure and adsorption capacity. These differences depend on the nature of the porous material (OG vs. CG), and, for a given set of materials, on the synthesis conditions of the OGs (Table 1). In the specific case of the OGs, N_2 isotherms corresponding to micro-/ mesoporous samples to non-porous samples were obtained (Figure 4a). This observation confirms the crucial role of the synthesis conditions in the final porous structure. Samples OG-5 and OG-18 exhibit a combination of type I and type IV isotherms due to combined presence of micro and mesoporosity, while the isotherm for sample OG-55 resembles type II, characteristic of non-porous materials. Interestingly, sample OG-5 exhibits capillary condensation at $p/p_0 \sim 0.50$ and sample OG-18 at $p/p_0 \sim 0.8$, i.e. the threshold pressure for capillary condensation in mesopores shifts to higher values with variations in the synthesis conditions. In the specific case of sample OG-55, although the nitrogen isotherm remains rather flat up to $p/p_0 \sim 0.90$ due to the limited content of micropores, a sudden increase in the amount of nitrogen adsorbed can be appreciated above this threshold pressure. This increase in the amount adsorbed close to condensation must be associated to the beginning of some capillary condensation in wider pores, although without a hysteresis loop. The presence of mesoporosity is easily identified in samples OG-5 and OG-18 due to the appearance of a significant hysteresis loop (type H1 and

H4, respectively). Once more, the absence of significant capillary condensation and a marked hysteresis loop in sample OG-55 could be attributed to the presence of wide mesopores and/or small macropores, the condensation of N_2 in these cavities being outside the evaluated relative pressure range (rather close to $p/p_0 \sim 1$).

Concerning the carbon xerogels (Figure 4b), nitrogen isotherms also reflect important differences in their porous network. In this specific case, all samples exhibit a rather similar microporous structure with a total micropore volume adsorbed close to 150 cm^3/g. The larger uptake at low relative pressures compared to OGs samples anticipates the development of new micropores during the carbonization. Differences among CG samples are mainly reflected in the mesoporous network. Similar to the OGs, important capillary condensation processes take place at mid-high relative pressures, the threshold pressure also changing with synthesis conditions CG-5<CG-18<CG-55. These results reflect that, after carbonization, the resulting CGs preserve the mesoporous network of the organic xerogels, i.e. the large cavities seems hardly altered. Only the microporous structure is modified due to the removal of volatiles during carbonization, thus giving rise to new micropores. Table 2 contains a summary of the textural parameters obtained.

Table 2. Textural parameters of the evaluated samples as determined by N_2 adsorption at 77K.

Sample	S_{BET} (m^2/g)	V_{TOTAL} (cm^3/g)	V_{micro} (cm^3/g)	V_{MESO} (cm^3/g)
OG-5	383	0.37	0.16	0.21
OG-18	370	1.05	0.16	0.89
OG-55	115	0.75	0.05	0.70
CG-5	560	0.43	0.19	0.24
CG-18	680	1.08	0.27	0.81
CG-55	638	0.85	0.25	0.60

Textural properties of the synthesized organic and carbon xerogels show that all samples synthesized are mainly mesoporous in nature ($V_{meso}/V_0 \sim 1.3$-14), with a BET surface area around 380 m^2/g, for the OG samples (except sample OG-55 with little microporosity), and around 560-680 m^2/g, for their carbon counterparts.

DFT calculations have been applied to the nitrogen data to ascertain the pore size distribution (PSD). Figure 5a and 5b shows the distributions obtained for the two series of samples after application of the quenched solid density functional theory (QSDFT method), considering slit-cylindrical pore geometry, and equilibrium model on carbon materials (software provided by Quantachrome Corp.) [18].

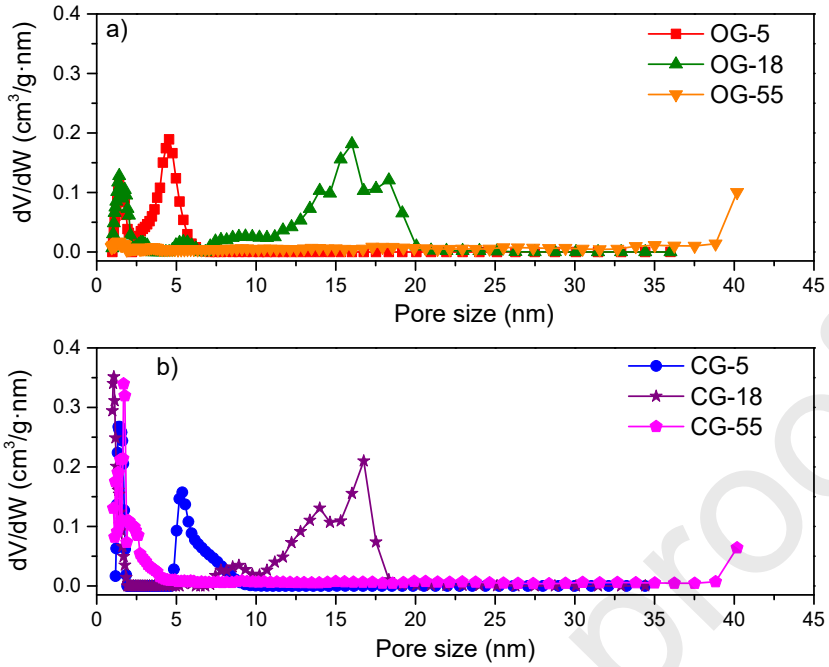

Figure 5. Pore size distribution obtained from the N_2 adsorption data at 77K for a) organic xerogels and b) carbon xerogels.

From the above results, it is evident that the porosity in the synthesized samples is quite homogeneous with a significant contribution of microporosity (below 2 nm), and an important contribution of mesopores. At this point it is important to highlight that these mesopores are rather homogeneous (narrow PSD), with maxima at around 5 nm, for samples OG-5 and CG-5, and at around 15-18 nm for samples OG-18 and CG-18. Samples OG-55 and CG-55 does not exhibit any maximum in the evaluated range (up to 40 nm), thus reflecting that mesopores in these samples, if any, must be wider. In summary, these results confirm the success in the synthesis approach applied to achieve mesoporous materials with a well-defined and controlled porous network. The similarity between OGs and CGs, in terms of mesoporous network, confirms that the carbonization treatment at high temperature does not alter this kind of pores. Furthermore, these results justify the selection of these two series of samples for a proper evaluation of the porous structure and surface chemistry at once in the hydrate formation process.

Hg porosimetry has been applied in order to complement the evaluation of the porous structure in the synthesized samples, mainly the evaluation of wider pores (Figure 6). Liquid mercury does not penetrate into pores below 4 nm, however, it is a very useful technique to probe larger mesopores and macropores. At this point it is important to highlight that organic xerogels could

not be evaluated properly using this technique since they suffer from serious deformations after the mechanical compression applied [19]. Concerning the carbon xerogels, Figure 6 shows that sample CG-55 exhibits a gaussian distribution with a clear maximum at 55 nm. Although N_2 adsorption data did not give valuable information about mesoporosity in this specific sample, Hg porosimetry data confirm the presence of mesopores above 40 nm and macropores (>50 nm), i.e., outside the range evaluated with the N_2 adsorption isotherms. In the specific case of sample CG-18, Hg porosimetry shows a well-defined PSD with a maximum at 18 nm, in close agreement with nitrogen adsorption data. Last but not least, for sample CG-5, the pore size is at the lower limit of the porosimetry technique. However, an amplification of the low pore size range (see inset) clearly denotes a maximum at around 5 nm, in close agreement with the N_2 adsorption data. As mentioned in the Experimental Section, the maximum of the distributions obtained using Hg porosimetry (in nm) were used for sample labelling.

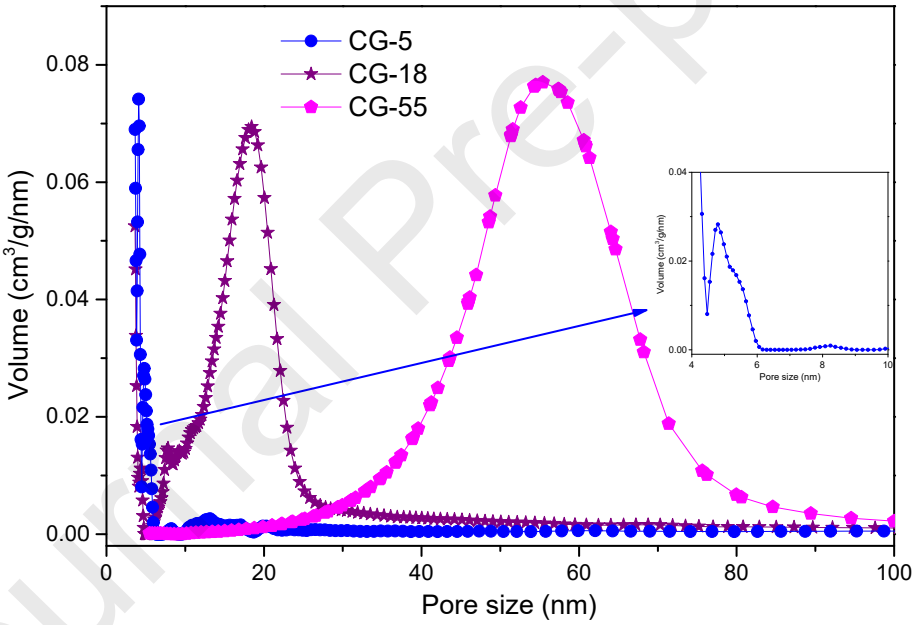

Figure 6. Pore size distribution of the CGs measured by Hg intrusion porosimetry.

The morphology of the synthesized samples was evaluated using field emission scanning electron microscopy (FESEM), Figure 7. The organic gels were not considered for evaluation since polymers present a low boiling point and the electron beam promotes their decomposition. As it can be appreciated in Figure 7, the mesoporous structure of the carbon xerogels depends on their morphology. Sample CG-5 with smaller mesopores looks more

compact and dense, whereas a wider network, with gaps and pores, can be appreciated for samples CG-18 and CG-55.

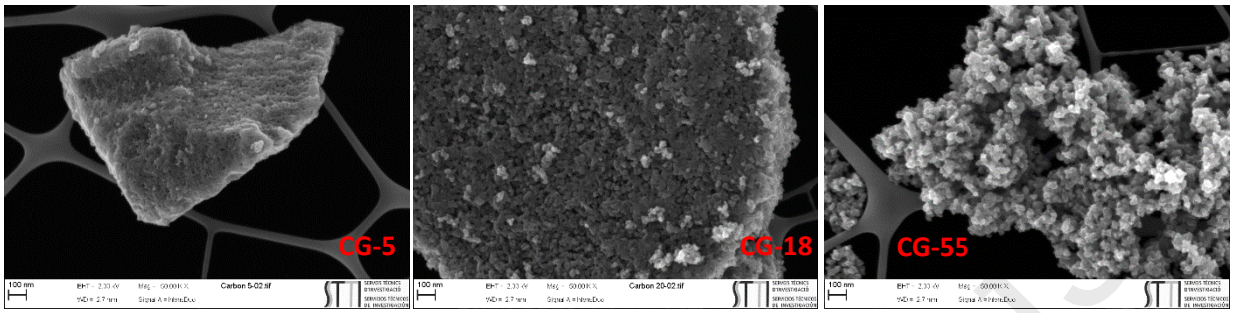

Fig. 7. FESEM images of the carbon evaluated samples.

The crystallographic structure of the synthesized samples (OGs and CGs) was evaluated using X-ray diffraction measurements. Figure 8 shows two representative examples of the XRD pattern for samples OG-5 and CG-5. The rest of the samples were not included because their XRD patterns looked rather similar.

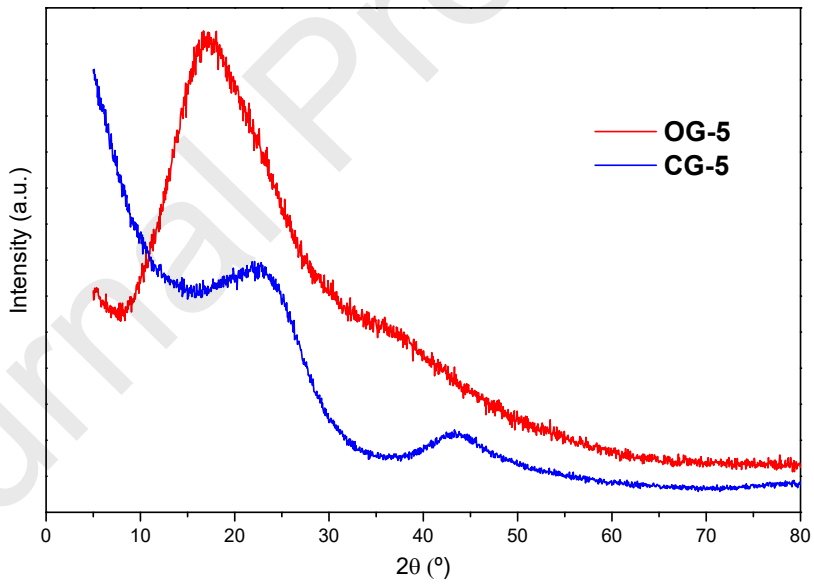

Fig. 8. X-ray diffraction patterns for two representative examples of organic and carbon xerogel.

Even though both samples show very low crystallinity, important differences are observed after the carbonization step. The organic xerogel shows some semi-crystallinity with a broad contribution centered at around 20º, indicating the presence of a partially ordered structure

coming from the aromatic rings. Once the sample is carbonized, this band disappears and two new contributions evolve at 23º and 43.6º, attributed to the (002) and (10) planes of graphite-like microdomains, respectively. Similar contributions in the XRD pattern have been described in the literature for activated carbons produced from biomass residues [20].

Another significant difference between OGs and CGs samples is their chemical nature, and indirectly, their surface chemistry. The analysis of the chemical composition is extremely important since it will define the adsorption performance towards polar molecules (e.g., H_2O) and their ability to promote or inhibit the methane hydrate formation process. The elemental composition is summarized in Table 3. As it can be observed, the main difference between organic and carbon xerogels concerns the amount of oxygen functionalities, and the associated carbon content. While the OGs exhibit around 40 wt.% oxygen, the carbonization treatment decompose all these groups (releasing volatiles), thus leaving behind a carbon rich structure (~ 95 wt.%), with a small contribution of oxygen functional groups (~ 2-3 wt.%).

Table 3. Elemental analysis composition (wt.%) of evaluated samples

sample	Nitrogen (%)	Carbon (%)	Hydrogen (%)	Oxygen (%)
OG-5	0	51.3	4.7	44.0
OG-18	0	55.1	4.2	40.7
OG-55	0	56.2	4.0	39.8
CG-5	0	95.4	1.5	3.1
CG-18	0	96.1	1.3	2.6
CG-55	0	96.2	1.4	2.4

Water adsorption isotherms at 298 K were measured to evaluate the hydrophilic/hydrophobic character of the synthesized samples (Figure 9). As expected from the elemental analyses (Table 3), organic gels are hydrophilic (type IV isotherm) and exhibit a large water uptake both at low relative pressures and at saturation ($p/p_0 \sim 1$). A closer look to these isotherms shows that water adsorption is quite significant at low relative pressures due to the presence of a rich surface chemistry (oxygen surface groups, see Table 3). In addition, all isotherms show a large capillary condensation above $p/p_0 \sim 0.5$ due to the capillary condensation in mesopores. The magnitude of this hysteresis loop decreases with the size of the mesocavities OG-5>OG-18>OG-55.

Although this result could be unexpected (based on previous Hg porosimetry measurements the mesopore cavities are larger for OG-55>OG-18>OG-5), it clearly anticipates that mesopores in samples OG-18 and OG-55 are too wide to promote complete water condensation at p/p_0 ~ 0.98. Contrary to the organic xerogels, carbon samples are hydrophobic in nature with a low adsorption capacity in the relative pressure range evaluated, also in agreement with their low oxygen contents (Table 3). Only above p/p_0 ~ 0.4 there is a certain amount adsorbed associated with a double hysteresis loop in the p/p_0 ~ 0.4-0.7 and p/p_0 ~ 0.7-1.0 regions. Although these two steps could be associated with water adsorption in micropores and mesopores, the total amount adsorbed is rather low compared to the total pore volume deduced from the N_2 adsorption isotherm. In other words, water is not able to condensate and fill the mesoporous network present in CGs.

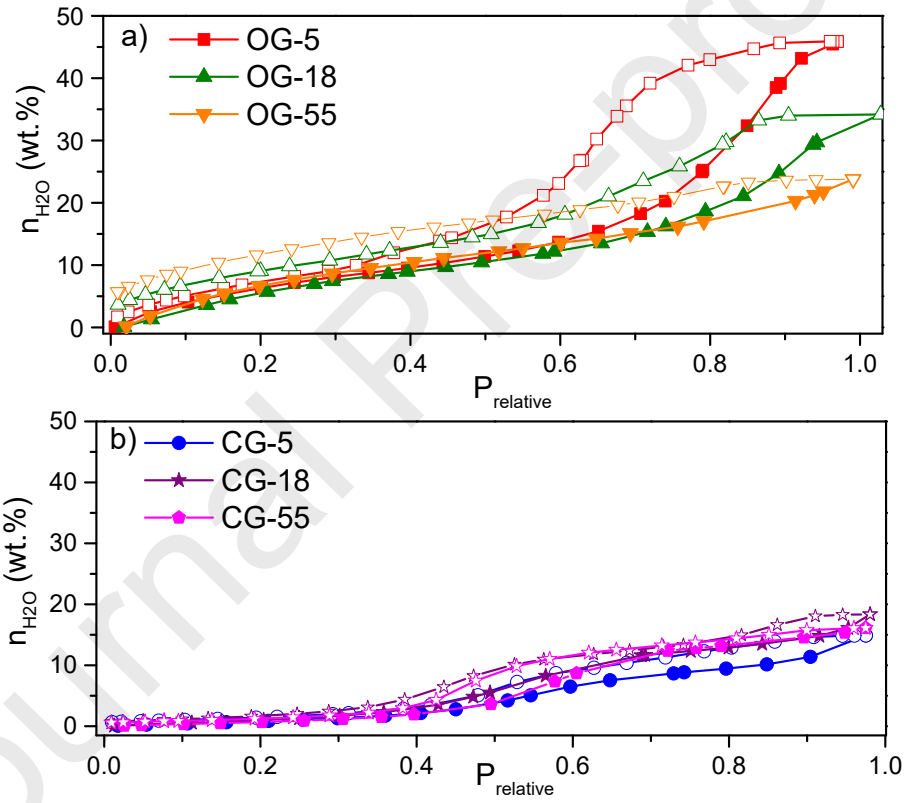

Fig. 9. Water vapor adsorption isotherm at 298 K for a) organic gels and b) carbon gels.

High-pressure methane adsorption processes in dry and wet conditions

Another important characteristic of these nanoporous samples is their methane adsorption capacity at high pressure and 275 K. It is well-known in the literature that under these experimental conditions methane is mainly adsorbed in micropores due its small diameter (ϕ_{CH4} = 0.38 nm) and the rather weak intermolecular interactions [21]. Figure 10 compares the excess

methane adsorption capacity for the organic and carbon xerogels up to 10 MPa under dry conditions. As it can be appreciated, independently of the nature of the host structure, all materials exhibit a type I adsorption isotherm, fully reversible over the whole pressure range evaluated. In general, the adsorption capacity of the CGs is much higher than that of their organic counterparts, in close agreement with the larger micropore volume reported for CG samples in Table 2. In this sense, the excess uptake at 10 MPa follows the order CG-18>CG-55>CG-5 with values around 6.66 wt.%, 6.35 wt.% and 5.36 wt.%, respectively. Concerning the organic gels, the order is slightly different OG-5≅OG-18>OG-55, with uptake values around 4.98 wt.%, 4.97 wt.% and 3.37 wt.%, respectively.

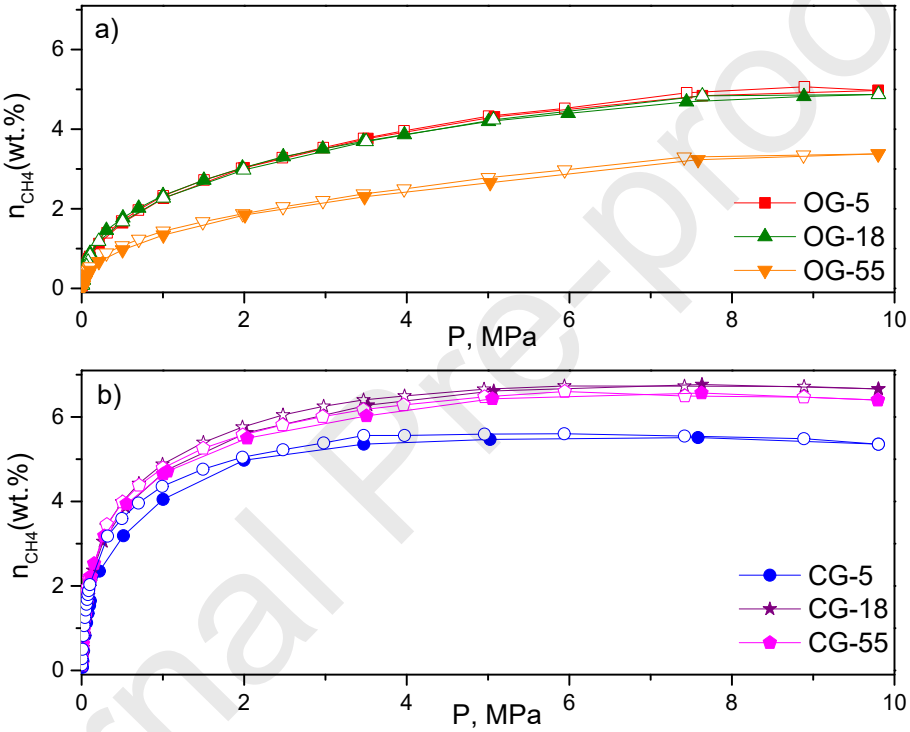

Figure 10. CH_4 adsorption isotherm at 275 K for a) organic gels and b) carbon gels.

The presence of a well-defined porous structure in the synthesized xerogels constitutes *a priori* an advantage to identify the role of the different pores in the methane storage process. Figure 11 reports the correlation between the excess methane uptake at 10 MPa and 275 K versus micropore, mesopore and total pore volume. As it can be observed, the correlation with the micropore volume is extremely good, with a correlation factor of 0.999 for the two sets of samples evaluated. Unfortunately, this correlation could not be preserved when comparing with the mesopore and total pore volume (mainly organic xerogels deviate from this tendency), thus reflecting that the micropores exhibit the major role in the methane adsorption process under these experimental conditions. However, the presence of a residual adsorption capacity of ~ 2

wt.% at a hypothetical V_0 = 0 cm^3/g suggest also some contribution (although less significant) from mesocavities.

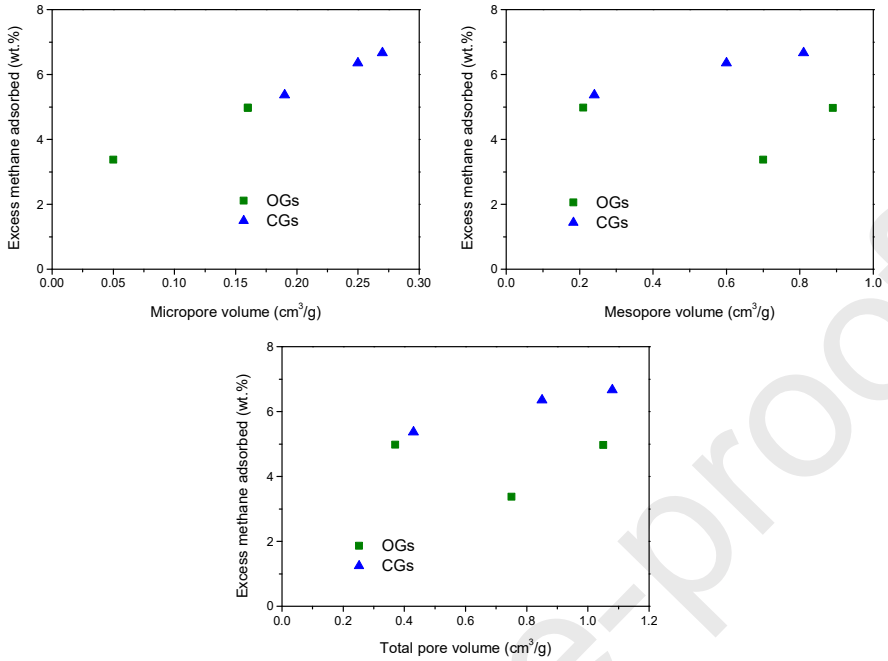

Figure 11. Correlation of the excess methane uptake at 10 MPa and 275K with the micropore, mesopore and total pore volume for organic (OGs) and carbon xerogels (CGs).

Once the dry samples have been evaluated, the high-pressure methane adsorption isotherms have been reproduced under water-supplying conditions, i.e. using the samples saturated with ultrapure water up to the total pore volume deduced from the N_2 adsorption isotherms (e.g., sample CG-18 with a total pore volume of 1.08 cm^3/g was impregnated with 1.08 g of H_2O per gram of sample under manual stirring until a homogeneous mixture is achieved). Figure 12 shows the high-pressure adsorption isotherms up to 10 MPa and 275 K. It is well-stablished in the literature that under these experimental conditions nano-confinement effects taking place in the inner porous structure can promote the nucleation and growth of confined nanocrystals with a higher yield and faster kinetics than natural or bulk hydrates [4].

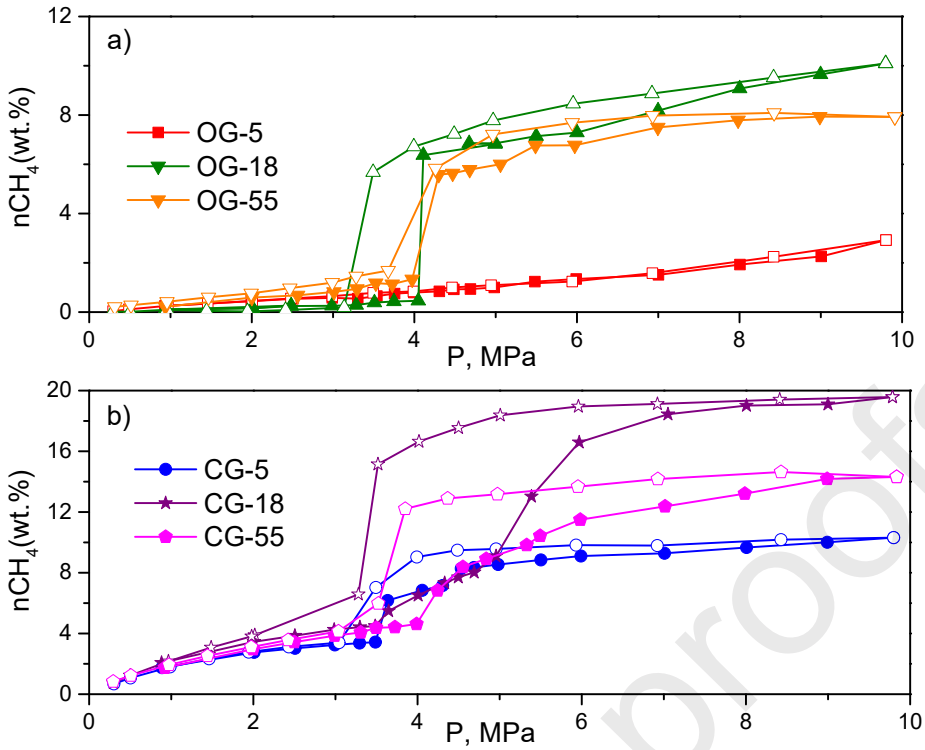

Figure 12. High-pressure CH_4 adsorption/desorption isotherms at 275 K for a) organic xerogels and b) carbon xerogels under water-supplying conditions.

The analysis of the high-pressure methane isotherms for the OGs show that below 4.0 MPa the three samples evaluated, OG-5, OG-18 and OG-55, exhibit a rather flat profile, i.e. the adsorption capacity for methane is very limited. This observation is rather different to the results described before for the dry OGs (Figure 10) and anticipates the presence of strong blocking effects by water pre-adsorbed in the inner porous structure. However, above a threshold pressure of ca. 4.0 MPa, methane adsorption isotherms exhibit a sudden jump up to a plateau at ca. 6-7 wt.%, the amount of methane stored increasing slowly afterwards up to maximum at 10 MPa of 8 wt.%, for sample OG-55, and 10 wt.%, for sample OG-18. Interestingly, the amount of methane adsorbed under wet conditions at 10 MPa is much larger than the values reported before for dry samples (up to 137% increase for OG-55 and 101% for OG-18). Previous studies described in the literature for activated carbon materials have shown that these drastic changes in the amount adsorbed in the high-pressure methane isotherms, and the associated hysteresis loop, reflects unambiguously the nucleation and growth of gas hydrates under confined environment [4]. Furthermore, the narrow pressure window for the hydrate formation and dissociation shown in Figure 12a suggests a uniform nucleation and growth, most probably associated with processes taking place in well-defined cavities. Based on the textural properties described in Table 2, one can anticipate that the hydrate nanocrystals could be grown in the large

mesocavities and small macrocavities present in these samples. Surprisingly, sample OG-5 with mesopores around 5 nm in size does not exhibit any significant adsorption up to 10 MPa. The rather flat profile is quite unexpected since previous studies using activated carbon materials have postulated that mesopores are optimum cavities to promote the hydrate formation, in terms of storage improvement compared to the dry system [13]. However, it is well-known in the literature that systems with strong water-framework interactions (highly hydrophilic) are not prone to promote methane hydrate formation [9]. Based on these premises, the observed results suggest that gas hydrate formation in organic xerogels is not a favorable process, in close agreement with their hydrophilic nature, except in samples with wide cavities (>5-10 nm), where water-framework interactions are minimized. From the amount of water incorporated during the pre-impregnation step and the total amount of methane adsorbed at 10 MPa, it is possible to estimate the stoichiometry of the obtained hydrate compounds (Table 4).

Table 4. CH_4 uptake for the evaluated samples at wet and dry conditions.

Sample	Dry conditions	Wet conditions	
	nCH_4 uptake (wt.%)	**nCH_4 uptake (wt.%)**	**Hydrate stoichiometry (1 CH_4· x H_2O)**
OG-5	4.98	2.92	-
OG-18	4.97	10.1	9.8
OG-55	3.37	7.92	10.8
CG-5	6.35	10.31	5.5
CG-18	6.66	19.57	6.2
CG-55	5.36	14.31	7.8

As it can be observed, the obtained stoichiometry for the hydrates formed in the organic xerogels is around 1 CH_4 · 9.8-10.8 H_2O. Assuming the natural stoichiometry (1 CH_4 · 5.75 H_2O), these results clearly reflect a large excess of water non-forming hydrate. In other words, assuming the natural stoichiometry, the water-to-hydrate yield in organic xerogels must not be larger than 60%. The limited yield in organic xerogels is in close agreement with the presence of a rather disordered structure of water molecules next to the surface, similar to those found with silica, not prone to participate in the methane hydrate formation process, i.e. non-freezable water [22].

The scenario is different for their carbon counterparts. As it can be observed in Figure 12, at pressures below 3.5 MPa all carbon samples perform rather similar with a certain amount

adsorbed (ca. 3-4 wt.%). Although this amount is much lower than the one obtained in dry conditions, it reflects that micropores are not fully blocked by pre-adsorbed water and physisorption can take place. Most probably, carbon materials exhibit two kinds of micropores, those directly linked to the mesopores, prone to be blocked by water pre-adsorbed in the mesopores, and those directly accessible from the external surface or macropores, susceptible to remain un-plugged. Above 3.5 MPa samples CG-5 and CG-18 exhibit a step in the amount of methane adsorbed, this step being shifted to larger pressures in the case of sample CG-55 (≈ 4.0 MPa). Above these pressures, all three samples exhibit a progressive increase in the amount adsorbed up to a plateau at 10.3 wt.% for CG-5, 14.4 wt.% for CG-55 and 19.6 wt.% for CG-18. In all three cases, the desorption branch exhibits a significant hysteresis loop, the extent of the hysteresis being proportional to the amount stored, i.e. to the extent of the methane hydrate formation CG-5<CG-55<CG-18. This tendency reflects that in addition to the role of the surface chemistry, the porous structure of the host and, more specifically, the pore size is a critical factor defining the extent of the water-to-hydrate yield. In fact, the stoichiometry deduced from the amount of water incorporated and the amount of methane adsorbed in the pressure range 3.5-10 MPa gives values really close to the theoretical value, 1 CH_4 · 5.5-6.2 H_2O, at least for samples CG-5 and CG-18. This observation suggests that water-to-hydrate yield must be close to 100% in these mesoporous carbon materials [23]. On the contrary, wider cavities (for instance in CG-55 with an average pore size diameter of 55 nm) does not promote complete conversion, with some of the water remaining un-reacted (stoichiometry 1 CH_4 · 7.8 H_2O). The comparison of the methane storage capacity at 10 MPa between the dry and wet CGs shows that the improvement achieved in wet conditions is around 62% for CG-5, 194% for CG-18 and 167 % for CG-55, i.e. a pore size around 18 nm must be close to the optimum value for the methane hydrate formation process. Although the uptake values obtained under water-supplying conditions constituted a large improvement compared to the pure physisorption process (up to 20 wt.% CH_4 uptake for CG-18 in the presence of water), these values are far below those reported in the literature for high-surface area activated carbon materials (~ 80 wt.%) and slightly smaller than to those reported for highly optimized metal-organic frameworks (~ 33 wt.%) [4, 9, 24]. Despite these uptake limitations in OGs and CGs samples, the presence of a well-defined porous structure and surface chemistry has been very useful to get additional insight into the methane hydrate formation process in confined environment.

CONCLUSIONS

The application of organic and carbon xerogels as a host structure to promote the methane hydrate formation shows that the porous structure and surface chemistry are crucial parameters

defining the total methane uptake and the water-to-hydrate yield. Under dry conditions, high-pressure methane adsorption scales up with the micropore volume, independently of the nature of the host structure and the surface chemistry. However, the scenario changes drastically under water-supplying conditions due to the associated improvement in the methane uptake through the nucleation and growth of gas hydrates. The water-to-hydrate yield is much larger in carbon xerogels compared to their organic counterparts. This observation is attributed to the stronger water-framework interactions in OGs, thus preventing complete conversion, i.e. water in close contact with the xerogel surface is non-freezable. On the contrary, the water-to-hydrate yield is close to 100% for the more hydrophobic carbon xerogels. In addition to the surface chemistry, the pore size is also critical defining these nucleation processes. Experimental results show that cavities in the mesoporous range (e.g., around 18 nm), independently of the chemistry of the host material, are optimum for a maximum enhancement in the amount of methane uptake under water-supplying conditions vs. dry conditions.

ACKNOWLEGEMENT

Authors would like to acknowledge financial support from the MINECO (projects MAT2016-80285-p and CTQ2017-87820-R). Principado de Asturias-FICYT-FEDER (Project PCTI-Asturias IDI/2018/000118) is also acknowledged. L.A. Ramírez-Montoya thanks CONACyT, México, for a post-doctoral grant (CVU No 330625, 2017)

REFERENCES

[1]. E. Dendy Sloan Jr, Fundamental principles and applications of natural gas hydrates, Nature 426 (2003) 353-359.

[2]. S. Thomas, R.A. Dawe, Review of ways to transport natural gas energy from countries which do not need the gas for domestic use, Energy 28 (2003) 1461-1477.

[3]. Y. Kuang, Y. Feng, L. Yang, Y. Song, J. Zhao, Effects of micro-bubbles on the nucleation and morphology of gas hydrate crystals, Phys. Chem. Chem. Phys. 21 (2019) 23401-23407.

[4]. M.E. Casco, J. Silvestre-Albero, A.J. Ramirez-Cuesta, F. Rey, J.L. Jordá, A. Bansode, A. Urukawa, I. Peral, M. Martinez-Escandell, K. Kaneko, F. Rodríguez-Reinoso, Methane hydrate formation in confined nanospace can surpass nature, Nature Commun. 6 (2015) 6432.

[5]. A. Celzard, J.-F. Mareche, Optimal wetting of active carbons from methane hydrate formation, Fuel 85 (2005) 957-966.

[6]. A. Perrin, A. Celzard, J.F. Mareche, G. Furdin, Improved methane storage capabilities by sorption on wet active carbons, Carbon 42 (2004) 1249-1256.

[7]. P. Mekala, P. Babu, J.S. Snagwai, P. Linga, Formation and dissociation kinetics of methane hydrates in seawater and silica sand, Energy Fuels 28 (2014) 2708-2716.

[8]. E. Andres-Garcia, A. Dikhtiarenko, F. Fauth, J. Silvestre-Albero, E.V. Ramos-Fernandez, J. Gascon, A. Corma, F. Kapteijn, Methane hydrates: Nucleation in microporous materials, Chem. Eng. J. 360 (2019) 569-576.

[9]. M.E. Casco, F. Rey, J.L Jorda, S. Rudic, F. Fauth, M. Martinez-Escandell, F. Rodriguez-Reinoso, E.V. Ramos-Fernandez, J. Silvestre-Albero, Paving the way for methane hydrate formation on metal-organic frameworks (MOFs), Chem. Sci. 7 (2016) 3658-3666.

[10]. L. Borchardt, M.E. Casco, J. Silvestre-Albero, Methane hydrate in confined spaces: An alternative storage system, ChemPhysChem 19 (2018) 1298-1314.

[11]. K.B. Yu, A.O. Yazaydin, Does confinement enable methane hydrate growth at low pressures? Insights from molecular dynamics simulations, J. Phys. Chem. C 124 (2020) 11015-11022.

[12]. A. Siangsai, P. Rangsunvigit, B. Kitiyanan, S. Kulorathipanja, P. Linga, Investigation on the roles of activated carbon particle sizes on methane hydrate formation and dissociation, Chem. Eng. J. 126 (2015) 383-389.

[13]. L. Borchardt, W. Nickel, M. Casco, I. Senkovska, V. Bon, D. Wallacher, N. Grimm, S. Krause, J. Silvestre-Albero, Illuminating solid gas storage in confined spaces - methane hydrate formation in porous carbons, Phys. Chem. Chem. Phys. 18 (2016) 20607-20614.

[14]. I.D. Alonso-Buenaposada, E.G. Calvo, M.A. Montes-Moran, J. Narciso, J. A. Menendez, A. Arenillas, Desiccant capability of organic xerogels: Surface chemistry vs porous texture, Microp. Mesop. Mater. 232 (2016) 70-76.

[15]. N. Rey-Raap, J. A. Menendez, A. Arenillas, RF xerogels with tailored porosity over the entire nanoscale, Microp. Mesop. Mater. 195 (2014) 266-275.

[16]. N. Rey-Raap, J. A. Menendez, A. Arenillas, Simultaneous adjustment of the main chemical variables to fine-tune the porosity of carbon xerogels, Carbon 78 (2014) 490-499.

[17]. F. Rouquerol, K.S.W. Sing, G. Maurin, J. Rouquerol, P. Llewellyn, Adsorption by powders and porous solids, Academic Press, Elsevier Ltd., 2012.

[18]. A.V. Neimark, Y. Lin, P.I. Ravikovitch, M. Thommes, Quenched solid density functional theory and pore size analysis of micro-mesoporous carbons, Carbon 47 (2009) 1617-1628.

[19]. N. Job, R. Pirard, J.-P. Pirard, C. Alié. Non intrusive mercury porosimetry: pyrolysis of resorcinol-formaldehyde Xerogels. Particle & Particle Systems Characterization 23 (2006) 72–81.

[20]. B. Manoj, A.G. Kunjomana, Study of stacking structure of amorphous carbon by X-ray diffraction technique, Int. J. Electrochem. Sci. 7 (2012) 3127-3134.

[21]. R.F. Cracknell, P. Gordon, K.E. Gubbins, Influence of pore geometry on the design of micropores materials for methane storage, J. Phys. Chem. 97 (1993) 494-499.

[22]. S. Liang, D. Rozmanov, P.G. Kusalik, Crystal growth simulations of methane hydrates in the presence of silica surfaces, Phys. Chem. Chem. Phys. 13 (2011) 19856-19864.

[23]. C. Cuadrado-Collados, A.A.A. Majid, M. Martínez-Escandell, L.L. Daemen, A. Missyul, C. Koh, J. Silvestre-Albero, Freezing/melting of water in the confined nanospace of carbon materials: Effect of an external stimulus, Carbon 158 (2020) 346-355.

[24]. C. Cuadrado-Collados, G. Mouchaham, L.L. Daemen, Y.Q. Cheng, A.J. Ramirez-Cuesta, H. Aggarwal, A. Missyul, M. Eddaoudi, Y. Belmabkhout, J. Silvestre-Albero, Quest for an optimal methane hydrates formation in the pores of hydrolytically stable MOFs, submitted.

Highlights

- Organic and carbon xerogels are promising platforms to promote confined hydrates.
- Hydrate formation yield depends on the porous structure and surface chemistry.
- Carbon xerogels with a poor surface chemistry exhibit a high conversion yield.
- Cavities around 18 nm give rise to the largest improvement in the methane uptake.